GT2016-56927 DRAFT

OIL-AIR FLOW BETWEEN THE CAGE AND INNER RACE OF AN AEROENGINE BEARING

Akinola A. Adeniyi[*]   **Hervé Morvan**[†]   **Kathy Simmons**

Gas Turbine & Transmissions Research Centre (G2TRC)
The University of Nottingham, Nottingham, NG7 2RD, UK

Email: akinola.adeniyi@nottingham.ac.uk   herve.morvan@nottingham.ac.uk   kathy.simmons@nottingham.ac.uk

ABSTRACT

In aeroengines the shafts are supported on bearings that carry the radial and axial loads. A ball bearing is made up of an inner-race, an outer-race and a cage which contains the balls, these together comprise the bearing elements. The bearings require oil for lubrication and cooling. The design of the bearing studied in this work is such that the oil is fed to the bearing through holes/slots in the inner race. At each axial feed location the oil is fed through a number of equispaced feedholes/slots but there is different number of holes at each location. Once the oil has passed through the bearing it sheds outwards from both sides into compartments known as the bearing chambers.

A number of studies have been carried out on the dynamics of bearings. Most of the analyses consider the contributions of fluid forces as small relative to the interaction of the bearing elements. One of the most sophisticated models for a cage-raceway analysis is based on the work of Ashmore et al. [1], where the cage-raceway is considered to be a short journal bearing divided into sectors by the oil feeds. It is further assumed that the oil exits from the holes and forms a continuous block of oil that exits outwards on both sides of the cage-raceway. In the model, the Reynolds equation is used to estimate the oil dynamics.

Of interest in this current work is the behaviour of the oil and air within the space bounded by the cage and inner race. The aim is to determine whether oil feed to the bearing can be modelled as coming from a continuous slot or if the discrete entry points must be modelled. A Volume of Fluid Computational Fluid Dynamics approach is applied. A sector of a ball bearing is modelled with a fine mesh and the detailed simulations show the flow behaviour for different oil splits to the three feed locations of the bearing thus providing information useful to understanding oil shedding into the bearing chambers.

The work shows that different flow behaviour is predicted by models where the oil inlets through a continuous slot compared to discrete entry holes. The form as speed of oil shedding from the bearing is found to depend strongly on shaft speed with the shedding speed being slightly higher than the cage linear speed. The break-up pattern of oil on the cage inner surface suggests smaller droplets will be shed at higher shaft speed.

Keywords: Aeroengine bearing, Annular flow, Oil systems, Oil shedding, VOF.

NOMENCLATURE

A_o Cross-sectional area of leaving oil (A_{oc}, A_{ob})[m^2]
A_s Jet spread area on the cage [m^2]
A_h Area on the feed hole [m^2]
D Bearing ball diameter [m]
g Acceleration due to gravity, [m/s^2]
H_c Film thickness on the cage, [μm]
J_c^*, J_o^* Jet spread length scale

---
[*]seconded from the University of Ilorin, Nigeria
[†]Address all correspondence to this author.

1

$\dot{m}_f$	Domain feed rate [kg/s]
$\dot{m}_o$	Outflow mass flow rate [kg/s]
$\dot{m}_p$	Mass flow rate through periodic planes [kg/s]
$\dot{m}_r$	Mass rate retained [kg/s]
Q_o	Outflow rate [m^3/s]
R_s	Radius of the shaft (inner-race) diameter [m]
t	Flow time [s]
$\overrightarrow{U}$	Flow speed [m/s]
V_o	Exit oil velocity to bearing/chamber [m/s]
V_s	Shaft linear speed at the inner race [m/s]
W_c	Width of the cage [m]
W_r	Width of the raceway [m]
X, Y, Z	Coordinates
Δx	Length scale [m]

Abbreviations

CFD	Computational Fluid Dynamics
VOF	Volume of Fluid

Greek symbols

α	Volume fraction
ω_c	Cage angular rotation, [rad/s, rpm]
ω_r	Raceway angular rotation, [rad/s, rpm]
Ω_s	Shaft rotation, [rad/s, rpm]
θ	Film extent, [rad, ^{o}]
ϕ	Level set function

INTRODUCTION

The purpose of the oil system in an aeroengine is for lubrication and cooling of transmissions elements including the shaft-supporting bearings. These highly rotating elements are housed within bearing chambers. The purpose of the bearing chamber is to contain the oil and an important aspect of chamber function is that the oil exits efficiently allowing quick recycling. The oil is used in a loop; the oil is pumped from the oil tank and fed to a bearing via its inner-race which has feed-holes and slots to get the oil into the bearing element interstices. The flow inside bearing chambers is complex and The University of Nottingham Technology Centre in Gas Turbine Transmissions Systems has been investigating such systems for some years.

The bearing chamber can be seen as an annular flow system in its simplest form. Flow in rotating concentric cylinders was first investigated in Taylor's [2] classical analytical work on simple rotating concentric cylinders encasing a viscous fluid. There have since been a number of significant investigations many of which are relevant to bearing chamber flow. A basic simplifying assumption in the mathematical models, is that the bearing chamber flow is a multiphase annular flow with the inside of the outer wall coated with a thin film driven by shear. This simplification has paved the way to significant progress in model development and system understanding. These so-called thin film mod-

els are based on lubrication theory with development for bearing chamber applications following chronolgically through Farrall et al [3], Williams [4], Kay et al [5] and Kakimpa et al [6]. Studies on more engine representative geometries, including [7–9] have investigated computationally the flow phenomenon inside the bearing chamber cavity. The recurring assumption in the models is that we understand the shedding characteristics of the oil from the bearing or in the simpler models, that the flow is a simple rimming flow. Experimental work such as those of Chandra et al [10] and Glahn et al [11] provide information on what happens to the oil after being shed from the bearings but little is known about the breakup process inside the bearing itself.

The work reported here is part of a larger study that seeks to provide understanding of what happens inside a bearing. One of the justifications for understanding the flow inside the bearing is the need for more accurate boundary conditions for our existing bearing chamber models as identfed by [8, 12]. In parallel research an experimental test facility has been constructed that will allow visualisation and other data acquisition relating to oil shedding from an aeroengine ball bearing. The configuration investigated computationally is intended to be as similar as possible to that of the experimental investigation.

Figure 1 shows a schematic representation of the test section of the bearing as configured in the test facility. The stub shaft is driven up to engine representative speeds by a motor and axial loads are applied via a large electromagnet. Oil is fed to the bearing via the inner-race at locations as shown in Figure 2 and exits into the front and rear chambers as shown. The test facility is instrumented and there is good visual access to the front chamber so that high speed cameras can be used to provide information about the exiting oil. There is no visual access to the bearing itself (the region marked in red on Figure 1) and limited opportunity for measurements also. The intention is that the CFD and experimental data together will provide a clearer picture of the flow into the bearing chamber from the bearing.

One of the challenges faced in modelling the flow inside the bearing itself is the complexity of the bearing geometry. As can be seen in Figure 2 the 25 bearing balls are positioned within a cage that restrains their motion and this creates some very small gaps within the model. Both the outer and inner races are also schematically illustrated in Figure 2. This figure shows the three feed routes to the bearing with the desired split of oil to these different locations being achieved through different numbers of feedholes as shown. In the example given here, there are 9 and 6 holes, respectively to the front and rear of the rig while 6 slots deliver oil to the mid-split of the inner-race.

To model the bearing, a periodic model is highly desirable as it reduces the computational overhead. The oil feed arrangement however creates a challenge for simplifying the model because the periodicity associated with the feedholes differs from that of a single ball element and also differs according to whether it is the front or rear location. With consideration for modelling a

single ball, a periodic domain of $14.4°$ is suitable but the feeds make this a little involved. It is therefore important to understand the behaviour of the feed system.

In previously reported modelling of this aeroengine bearing Adeniyi et al [13] simplified the feed arrangement by representing it as a continuous slotted feed. However, although some relevant and useful data was obtained, concerns remained as to the validity of this simplification. In the work reported in this paper, modelling focus is on a region within the overall bearing model focussing on the feed arrangement and geoemetry immediately surrounding. The aim of the work is to better establish whether it is truly valid to model oil feed to a bearing that comes via discrete inlet holes as a continuous slot feed.

BEARING ELEMENT AND FLUID DYNAMICS

The elements of a roller bearing interact in a complex way. There is wide body of work on bearing dynamic analysis with a range of different simplifying assumptions. Work on the dynamic analysis of a bearing, including consideration for the lubricant probably finds its roots in the 1978 work of Kannel & Walowit [14]. However the ADORE bearing analysis software (Gupta [15]), one of the most significant tools available to the bearing designer owes most to Gupta who developed the original commercial code and has a body of work too large to reference it all. The basic assumption in the dynamic models is that the fluid forces are generally small compared with the interaction forces of the bearing elements. In describing the hydrodynamic influence, a Reynolds equation formulation is solved. In the formulations, the fluid (oil) is taken as single phase in the domain, for example between the cage and inner race and at the contact points [1, 15].

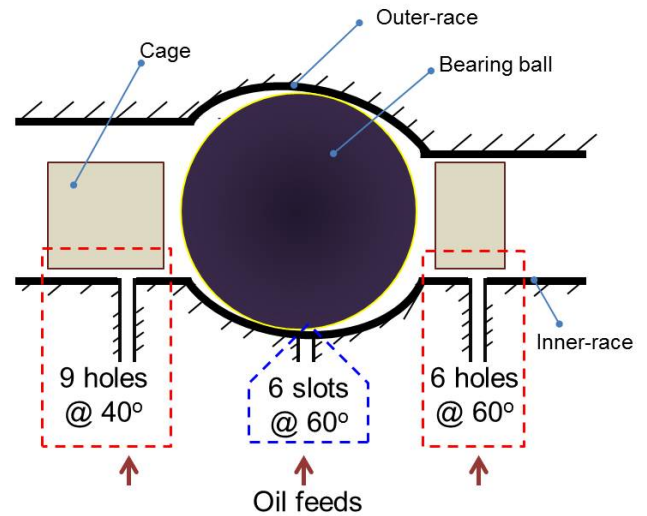Ashmore et al. [1] made modelling progress by assuming

FIGURE 1: SCHEMATIC REPRESENTATION OF BEARING IN TEST FACILITY

FIGURE 2: UNDER-RACE OIL FEED

that the cage-raceway can be considered to be a short journal bearing divided into sectors by the oil feeds providing hydrodynamic support for the cage. In the work presented in this paper, following Ashmore et al. [1], the cage-race is assumed to be relatively unaffected by the bearing balls such that the flow can be studied in isolation but unlike their work, the 3D Navier-Stokes equations are solved with consideration for the oil-air interface.

In the analysis of rolling element bearings there are essentially two approaches: quasi-static; and dynamic [1, 15–17]. In quasi-static analysis, for each of the bearing elements, the force and moment equilibrium equations acting are modelled such that they include the dynamic components such as the externally applied forces, centrifugal forces and gyroscopic moments. These result in a set of non-linear algebraic equations that require numerical techniques such as Newton-Raphson methods to solve and from which, angular velocities of the elements can be calculated. Jones [16] was among the first to analyse the motion of a high speed ball bearing using a simplified quasi-static analysis of ball motion with sliding friction but without the contributions of the lubricants. The quasi-static approach, in essence, represents steady state conditions and the raceway control assumption is used.

Raceway control is an assumption of non-gross slip at the contacts, so that the ball motion about its own axes as well as the bearing axis is controlled by the raceway and only rolling motion occurs [18, 19]. In the raceway control hypothesis, it is assumed that the balls roll relative to the controlling raceway but roll and spin with respect to the non-controlling raceway. In the formulation, the gyroscopic moment acting on the ball has a resisting frictional force on the controlling race with no gyroscopic slippage. Raceway control is not realistic as it is not possible
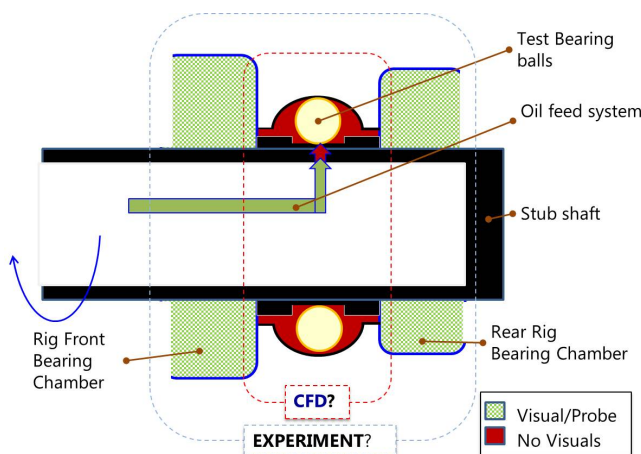
that only pure rolling exists at non-zero contact angle at either of the races. It is, however, useful to estimate steady state results [18, 20]; Wang et al. [21] recently proposed a technique to remove the raceway control assumption.

The dynamic analysis is a real-time representation of the bearing and does not require any kinematic contraints as required in quasi-static analysis. In the dynamic models, the equilibrium equations from the quasi-static model are formed using differential equations of motion for each of the bearing elements [15,22].

The Cage-Raceway Analysis

The focus of this paper is the cage-race part of the bearing. The model of Ashmore et al. [1] of the cage-raceway is illustrated in Figure 3. In the figure, there is an eccentricity, e as shown by the offset centres O_r and O_c for the raceway and cage respectively. The raceway speed is ω_r and the cage speed is ω_c. The oil from the feedholes forms blocks of oil exiting outwards and spreading to extents $\theta_1 - \theta_2$.
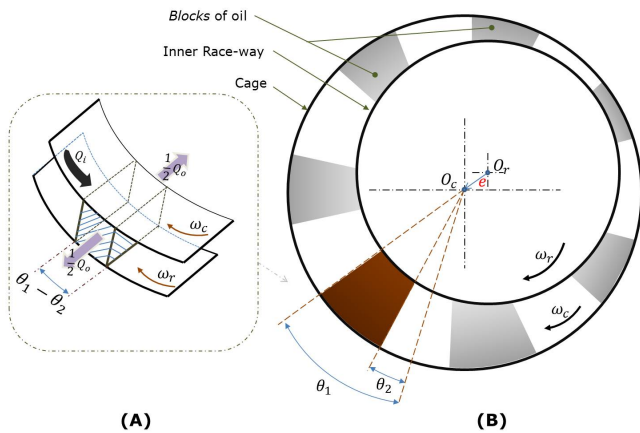
FIGURE 3: ILLUSTRATION OF THE MODEL OF ASHMORE ET AL [1] FOR AN OIL-FED CAGE-RACEWAY

The speed of the inner-race is the same as that of the shaft unless there is any undesirable slipping between it and the shaft. In this work slip is assumed not to take place. The speed of the cage can be estimated from the analysis of the rolling element interaction. This was not felt to be necessary for this study and instead the cage speed was chosen on the basis of estimations obtained from [18, 20]. In the current analysis, the cage is taken to be concentric with the shaft.

The fluid dynamics

The main focus of this work is the behaviour of the oil in the cage-raceway geometry. A computational fluid dynamics (CFD) approach is used to understand the flow of oil and air. A simulation of the entire $360°$ geometry would be expensive to achieve because of the length scales and computational mesh resolution involved. Instead, from the frame of reference of the oil feed, the flow is solved as a periodic flow based on the physical spacing of the holes. The effect of gravity on the fluid within the width of the raceway is considered negligible as the centrifugal force overrides (ie $\Omega_s^2 R_s/g >> 1$)). The continuity equations and Navier-Stokes equations are solved isothermally.

THE MODEL SETUP
The Geometries

Figure 4 shows one of the geometries used in the simulations in this work. The chosen periodicity planes are shown. One of the periodic geometries has periodic planes spaced $40°$ apart and the other has $60^c irc$. The width and diameters are the same in both cases. The diameter of the feed holes (D_h) is $1.76mm$, as was the case in Ashmore et al. [1]. A fixed annular spacing of $0.22D_h$ between the inner-race and the cage inner-wall is used. The widths of the cage (W_c) and the raceway (W_r), as used in the simulation, are $6.14D_h$ and $3.81D_h$ respectively. The geometry is not symmetric about the feed as can be seen in Figure 6. There is a small fillet radius on the cage at the side furthest from the rolling element.

In another of the cases investigated, the feed holes were replaced with slotted feeds at a periodicity of $14.4°$ (ie one slot per ball). In all cases, holes and slots, the feeds deliver same total amount of oil. There are many ways to choose the width of an equivalent slot; but in this paper, the widths chosen are 10% and 20% of the feed hole diameter.

For a qualitative comparison, a $360°$ geometry with one feed hole was created, as illustrated in Figure 5. This removes the periodicity assumption. In this case, the geometry is radially split into two zones. The zone with the feed rotates and the non-rotating zone is in another frame of reference with a sliding interface between the two zones.

The Computational Mesh

A structured mesh (ANSYS-ICEM Hexa Mesh) is used in the periodic geometry setups as illustrated in Figure 6. There is a better control over the number of cells as well as better nodal-mesh spacing efficiency in a Hexa mesh compared to unstructured meshes but the latter are easier to construct for more complex geometries. The setups with periodicity are straight forward to construct using ICEM "logical blocking" except for the sub-millimeter gap sizes that require the use of very small cells to provide sufficiently high resolution.
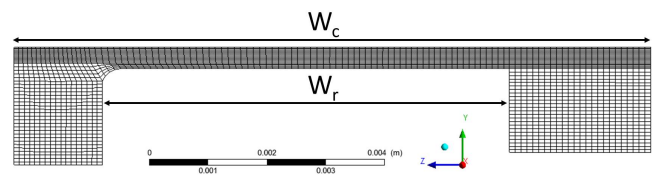
The rotating setup requires the use of a sliding mesh plane. The sliding plane is a plane of zero-thickness separating the two fluid zones. This is built by creating two fluid zones one either

4
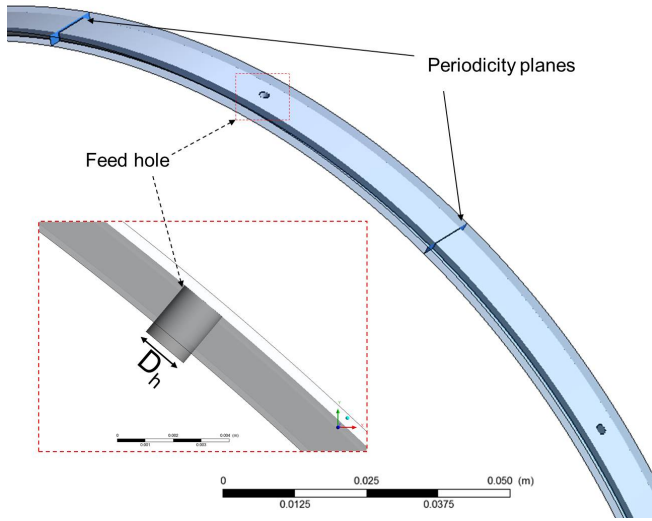
FIGURE 4: CAGE-INNER RACE PERIODIC GEOMETRY
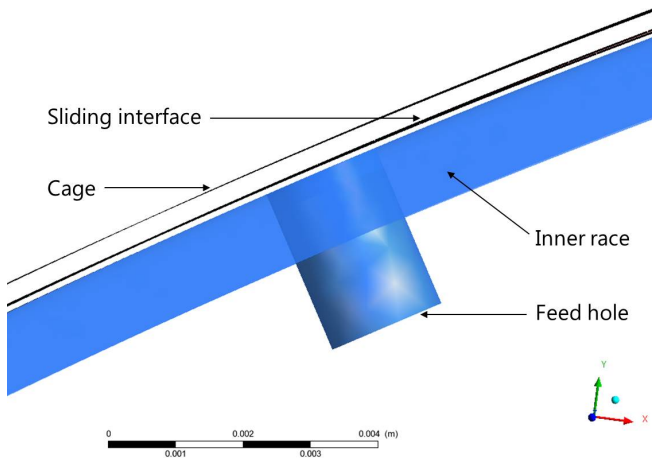
FIGURE 5: CAGE-INNER RACE FULL 360° ROTATING GE-OMETRY

FIGURE 6: BEARING OIL SHEDDING RIG

side of the sliding interface. The total size of mesh is largely determined by the number of cells in the gap between the inner-race and the cage. Two meshes with 14 and 20 cells across the gap have been used in this paper to provide an amount of mesh depen-

dence study. These resulted in meshes of $235,000$ and $1,500,000$ cells. The mesh size in the $360°$ geometry is about 4.2 million cells.

The solution method

The coupled level set volume of fluid (CLSVOF) technique as proposed by Sussman & Puckett [23] and implemented in AN-SYS Fluent [24] is used in this work. In the volume of fluid (VOF) technique, a colour function, α, is solved to describe the oil-air mixture. Where the volume fraction is 1, the domain is completely filled with oil and if $\alpha = 0$ it is completely air filled. The free-surface is in the region $0 < \alpha < 1$. The level set approach uses a smooth signed function, ϕ such that a zero level set iso-surface represents the free-surface and a positive or negative level set describes either phase of the mixture. The SST $k - \omega$ turbulence model was used; this model has modifications to resolve low Reynolds number [24].

The timestep, Δt, for the simulations is of the order $0.1\mu s$ chosen by keeping the CFL number (Courant-Lewy-Freidrich number, $CFL = |\overrightarrow{U}|/(\Delta x/\Delta t))$ less than 1; where Δx is the mesh size length scale and $\overrightarrow{U}$ is the flow speed. Keeping CFL less than 1 is essential for solution stability for the explicit transient VOF formulation used. The second order accurate upwind differencing scheme is used for the spatial terms of the continuity and the momentum equations. First order accurate explicit time integration is used for the temporal terms while convergence criterion set for the residuals is 10^{-4} and a maximum of 30 iterations per time step. The simulations were run using 8 cores on 4 machines with 16 GB RAM per machine on the University of Nottingham's high performance computing cluster. The simulations run $1.1\mu s$ flow time per CPU compute hour for the $360°$ rotating setup, while the periodic setups take between 8 and $110\mu s$/CPU-hour.

To monitor the flow for steady state behaviour, the residual mass flow within the system is monitored. Consider the system of flow schematically given in Figure 7. The 3D control volume is represented with the dashed lines.

The system is fed (through hole or slot) at the rate of $\dot{m}_f$. By definition the flow into the system through the periodic boundaries matches the flow out and this is represented as $\dot{m}_p$. The oil mass flow through the "chamber side" and "bearing side" boundaries of the domain is represented as $\dot{m}_{o1}$ and $\dot{m}_{o2}$ respectively and the rate of mass retention within the system is $\dot{m}_r$. Mass conservation of the system in Figure 7 is given by Eqn. (1a). Steady state is expected when Eqn. (1d) can be satisfied. Equation (1c) is expected to fluctuate and then approach a continuous straight line. The flows are checked qualitatively to be seen to be steady and as well satisfy the steady state criterion given here.

5

$$\dot{m}_f + \dot{m}_p = \dot{m}_{o1} + \dot{m}_{o2} + \dot{m}_p + \dot{m}_r \tag{1a}$$

$$\dot{m}_r = \dot{m}_f - (\dot{m}_{o1} + \dot{m}_{o2}) \tag{1b}$$

$$\frac{\partial m_r}{\partial t} = \frac{\partial}{\partial t}\left(m_f - [m_{o1} + m_{o2}]\right) \tag{1c}$$

$$\frac{\partial m_r}{\partial t} \approx 0 \tag{1d}$$

Boundary Conditions

The inner-race and the feed hole pipe are merged as a single entity named "inner-race". The cage and the inner-race are specified as no-slip wall boundaries. The walls are specified as "moving walls" with their respective angular velocities. To use the frame of reference of the feed, the inner-race angular velocity is set as 0 *rpm* and the cage's relative angular velocity is the difference between its and those of the inner-race. The exits into the bearing chambers are pressure boundaries in all cases. The inlet of the feed holes are specified as velocity inlets with the velocity specified as normal to the inlet. Periodicity is imposed on the locations as indicated in Figure 4.

Total bearing oil flow rates of 8 and 10 litres per minute (1.33×10^{-4} kg/s and 1.66×10^{-4} kg/s were investigated for 5,000 and 10,000 rpm shaft speeds. These are typical values within the aerospace context. The cage speeds used are 2,658 rpm (for shaft speed 5,000 rpm) and 4,985 rpm (for shaft speed 10,000 rpm).

RESULTS

Table 1 gives the matrix of the cases that have been run. The case nomenclature is such that those starting with S refer to the cases with slotted feed, Q refer to the feed through a hole in the race with 40° separation and H for hole feed with 60° separation
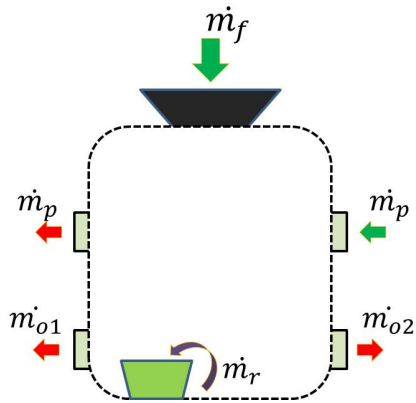

FIGURE 7: FLOW MONITOR

while $F1$ is the case with 1 rotating oil feed. Case Q1 is the one with 14 cells in the cage-race gap others have 20 cells in the gap.

TABLE 1: CASES SIMULATED

Case #	Type	Ω_s(rpm)	Bearing oil feed rate (ltr/min)
S1	$0.1D_h$	10,000	10
S2	$0.2D_h$	10,000	10
Q1	$40^o/14$	5,000	8
Q2	40°	5,000	8
Q3	40°	5,000	10
Q4	40°	10,000	8
Q5	40°	10,000	10
H1	60°	5,000	10
H2	60°	10,000	10
F1	360°	5,000	8

Mesh dependence

A full mesh independence study has not been conducted for this modelling work because it builds largely on work previously reported [13]. The only parameter investigated was the number of cells across the gap between inner race and cage. It was concluded that 14 cells were insufficient and all the cases were run with 20. Within the timeframe of this investigation it was not feasible to compute with more.

Qualitative Analysis

For the cases where oil is supplied through a feed hole, it was found that far from running full, the oil accelerates radially outwards and forms a fast moving thin film on one side of the hole. This is illustrated for case H2 by the oil iso-surface in Figure 8. As can be seen there is a recirculation of air in the pipe cavity; with the pipe inlet oil only, air cannot come through the hole but in an actual bearing this may not necessarily be the case throughout the 360° rotation. Moving into the gap between inner race and cage the oil can be seen to collect on the underside of the cage but again the film is thin and so it does not extend to the inner race. This behvaiour is consistent in all cases with the hole feed. If in reality the oil does not fill the space between the cage and the raceway then this would suggest the oil will hardly provide any hydrodynamic support to the cage.

6
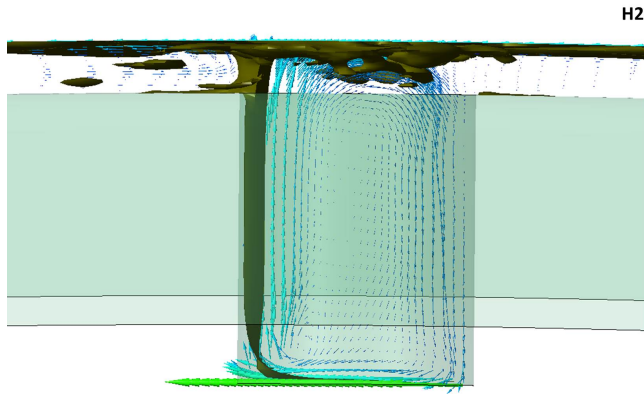
FIGURE 8: OIL IN THE FEED PIPE

Figure 9 shows the oil film on the inside wall of the cage (viewed from above the cage as if transparent). The red patches show the oil as this is where there is a volume fraction of 1. Shaft rotation is counter-clockwise in these figures. The jet of oil from the feed can be seen to generally form a star shaped area of impact. As expected, the oil exits to the both sides axially. An interesting feature of the results obtained is that for the cases of shaft speed 10,000 rpm (Q4, Q5 and H2) it can be seen that the oil trail on the cage breaks into discrete oil patches very reminiscent of jet breakup into droplets caused by Rayleigh-Plateau instability. This is true for both feedrates investigated but this behaviour is not seen for the cases of shaft rotatation at 5,000 rpm. All the subfigures of Figure 9 show that there is little interaction of the oil from any neighbouring oil feeds for either the 40° (Q) or 60° (H) feed spacing.

A conclusion from this study is that oil exiting the bearing into the bearing chamber from the location between cage and inner race will enter the chamber not as a sheet of film but rather as discrete "chunks" of oil. At the lower shaft speed of 5,000 *rpm* the axial spreading from the feed would lead to ligaments/droplets entering the bearing chamber. At the higher shaft speed of 10,000 *rpm* there is disintegration of the feed over the cage suggesting smaller droplets would be shed.

Comparison with the case with the single rotating feed on a 360° geometry is shown in Figure 10. The oil behaviour is consistent with the periodic case Q2 confirming the validity of the periodic modelling approach.

The behaviour of the flow in geometries with the slotted feed (cases S1 and S2) is quite different from the ones with a hole feed. Figure 11 illustrates the results obtained for one of the slot feed cases. Figure 11A shows a continuous film on the lower surface of the cage; the film is fairly uniform and almost the entire surface is wetted. Figure 11B can be compared to Figure 8 and shows that in this case too the film does not fill the cavity but forms a film under the cage that is shed into the chamber and
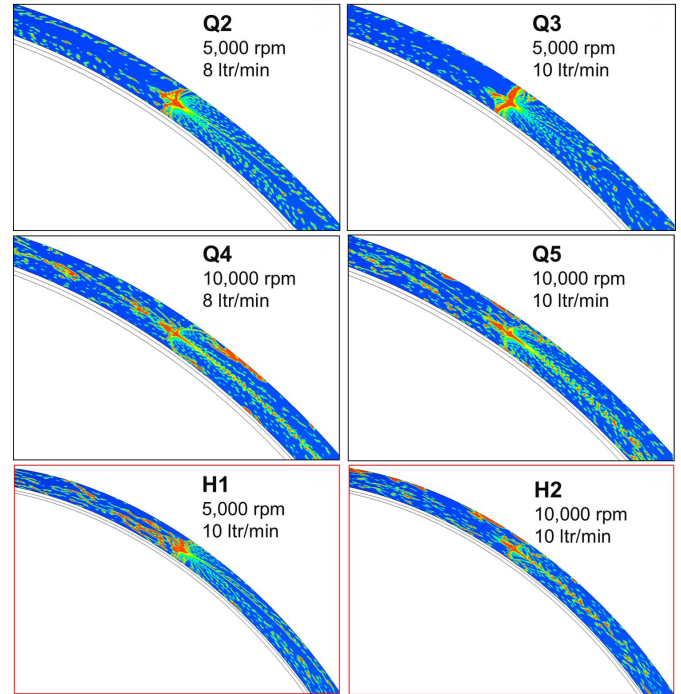
**FIGURE 9**: OIL WETTING OF THE CAGE FOR THE SECTOR MODELS
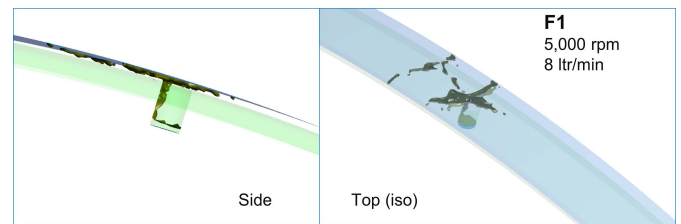
FIGURE 10: OIL BEHAVIOUR IN HOLE AND ON CAGE FOR 360° CASE

bearing. Because of the extent of the film on the lower surface of the cage, these results suggest that for feed slots the oil emerges as a sheet of oil.

For both the slotted feed and hole feed, in no case did the oil fill the cavity despite the small gap between the cage and inner race. Granted there is no eccentricity of the cage with respect to the inner race in these models but the finding is nevertheless of interest.

Quantative Analysis

The results from the simulation were post-processed using ANSYS CFD-Post. One of the purposes for this work was to better understand the behaviour flow from the oil feed with the hope that it is possible to find a simpler but representative method
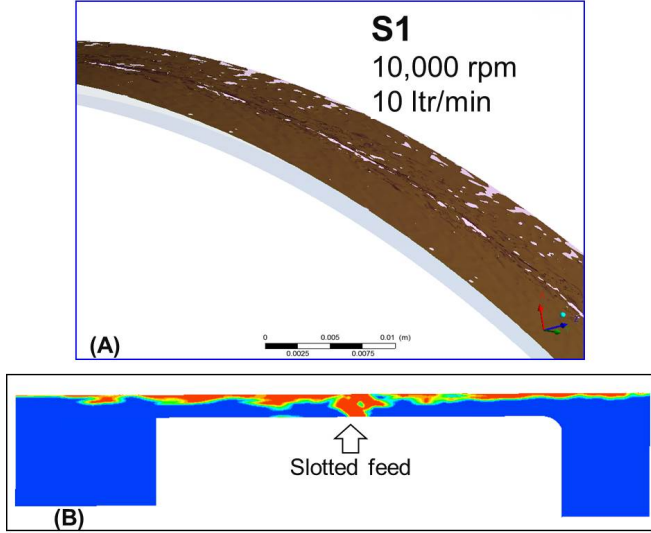
FIGURE 11: CAGE OIL WETTING FROM A SLOTTED FEED

of represent the oil feed in a bearing model. The behaviour of the oil jet during impact on the cage as well as the oil exit from both sides of the gap between cage and inner race are presented here.

One of the parameters identified as of interest is the extent of oil spreading on the cage inner surface. This is expressed using the ratio of the wetted area A_s on the cage (the area before any disintegration) divided by area of the feedhole (A_h):

$$J_c^* = \sqrt{A_s/A_h} \qquad (2)$$

A second parameter relates to the area of oil ligament/filament leaving the cage inner surface (it is effectively a measure of film thickness and angular extent) on the chamber side A_{oc} or bearing side A_{ob}. In this case the non-dimensional parameter is:

$$J_o^* = \sqrt{A_o/A_h} \qquad (3)$$

To post-process/extract the area of interest, an "iso-clip" is created using a macro based on the volume fraction of oil ($\alpha \geq 0.5$) and the coordinates of the feed hole. With this iso-clip, the oil exiting the geometry directly from the jet can be directly analysed.

Figure 12 shows the spread parameter J_c^* for the cases where oil is fed through a hole with $40°$ periodicity (Q1-Q5). The spread is between 3 and 5 times the size of the feed hole. The spread generally increases with the shaft speed (comparing cases

Q1-Q3 to cases Q4-Q5). For a fixed speed the spread reduces with increasing flow rate (comparing Q2 to Q3, Q4 to Q5). For the cases where oil is fed through a hole with $60°$ periodicity (cases H1-H2), the spread reduces with increased shaft speed. This figure gives an idea of the instantaneous wetting of the lower surface of the cage.
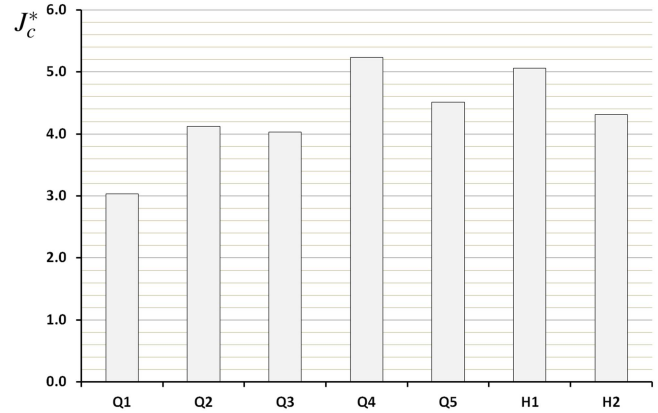
FIGURE 12: OIL SPREAD ON THE CAGE

The parameter characterising the oil shedding from the cage into the chamber or bearing (J_o^*) is given in Figure 13. The most immediately notable aspect of Figure 13 is that shaft speed differentiates behaviour as can be seen by comparing cases Q1-Q3 with Q4-Q5 and H1 to H2. At $5,000$ rpm the shedding parameter is around 0.2 whereas at $10,000$ rpm the shedding parameter is around 0.7. For the two oil flowrates investigated flowrate makes little difference (comparing Q2 to Q3, Q4 to Q5). In cases Q2 and Q4 the flowrate is the same but the shedding parameter differs significantly and this indicates that the oil is shedding at higher speed when the shaft speed is higher. The shedding parameter is similar here for both bearing and chamber sides of the cage indicating fairly even split although it should be recalled that the geometry investigated here is far less representative of the bearing side in the actual bearing. This CFD data shows that, as might be expected, shedding speed depends primarily on shaft speed. The data also shows that because films are thinner at higher speed (increased spreading parameter J_c^* the shedding speed increases more than linearly with shaft speed (ie J_o^* at $10,000$ rpm is more than twice J_o^* at $10,000$ rpm)

To investigate this further the mean velocity of the oil (filaments) as they exit is given in Figure 14 for the various cases. The effect of shaft speed is clear. For comparison, at shaft speed $5,000$ rpm the cage speed is $2,658$ rpm giving a cage linear speed ($r\omega$) of 34.5 m/s and for shaft speed $10,000$ rpm (cage speed $4,985$ rpm) the cage linear speed is 65.3 m/s. Figure 14 shows that oil mean exit velocity is a little higher than cage linear speed,
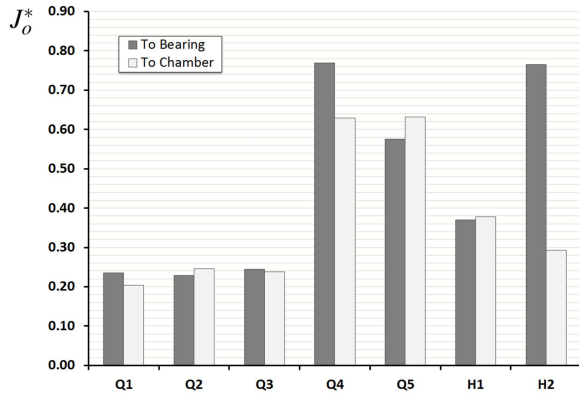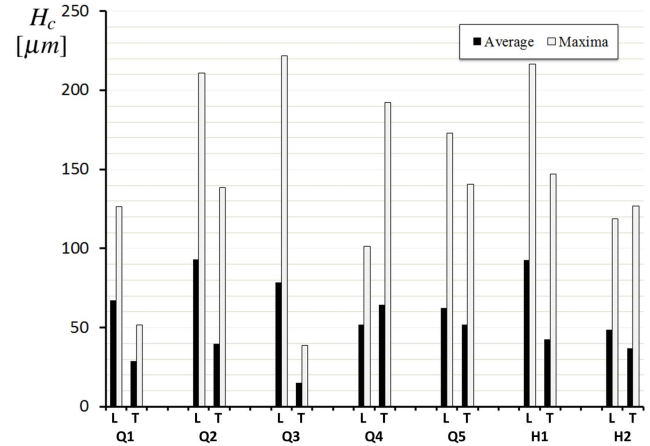
8

FIGURE 13: OIL EXIT SIZE FACTOR

FIGURE 15: JET LEADING/TRAILING FILM THICKNESS

and this will be as a consequence of the axial velocity component. For the two oil flowrates investigated there is very little difference in mean oil shedding velocity. There is also very little difference between the cases for 6 holes and 9 holes ($40°$ sector and $60°$ sector).
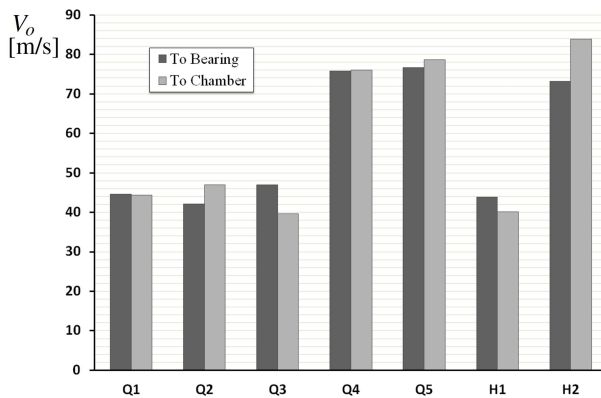

FIGURE 14: EXIT OIL VELOCITY

The film thickness was measured in front of the jet as well as behind the jet and the data is shown in Figure 15. The measurement in front of the jet is marked as L (leading) and behind is marked as T (trailing) in the figure. The figure shows the average and maxima of the film thickness under the cage for the feed hole simulations. The film is thicker in front of the jet impact and thinner trailing the jet motion. The film thickness is less than $250 \mu m$ in the wetted part of the cage. The film thickness is similar for all the flow rates. The mean film thickness for the slotted feed case are 124 and $118 \mu m$, respectively for the cases S1 and S2.

CONCLUSIONS

In this work, a numerical simulation was made for the oil/air flow in the region of an previously investigated aeroengine bearing between the inner race and the cage. This region is characterised by a very narrow annular gap. The work aimed to establish whether the oil feed obtained on the actual bearing via holes through from under-race feed could be represented by a continuous slot input. As the feed-holes are periodically spaced, advantage was taken to use periodicity with a frame of reference centred on the inner race. Simulations were obtained for two shaft speeds, $5,000$ rpm and $10,000$ rpm, and two oil flowrates, 8 and 10 litres per minute, these being typical values for the bearing of interest.

Results from the simulations with oil supply through feed holes show that the oil does not fill the entire feed hole. After leaving the feed hole the oil forms a wetted area on the inner surface of the bearing cage, spreading and shedding to both sides. In none of the cases investigated was the annular gap full of oil. The wetted area on the cage was investigated and no consistent pattern of variation with shaft speed or oil supply flowrate was found; in all cases this area was 3-5 times the area of the exit hole. The cross-sectional area of flow shedding from the bearing was a strong function of shaft speed as was the speed of the oil at point of shedding. This latter was found to be slightly higher than the linear cage speed. The oil on the cage breaks up into smaller wetted areas that ultimately shed as ligaments, filaments and droplets. The oil filaments are more regular at the $5,000$ rpm speeds and more disintegration was found at $10,000$ rpm for both oil flow rates investigated suggesting that smaller droplets would be shed.

Results from the simulations with oil supplied through a continous slot show an even, almost continuous coverage of film on the cage inner surface. The average film thickness for slot feed is around $120 \mu m$ whereas for feed through holes the aver-

9

Copyright © 2016 by Rolls-Royce

age film thickness is far less, typcially in the range $50 - 90\mu m$.

It is concluded that discrete feed through oil feed holes and continuous feed through a slot input do not yield comparable results.

REFERENCES

[1] Ashmore, D. R., Williams, E. J., and McWilliam, S., 2003. "Hydrodynamic support and dynamic response for an inner-piloted bearing cage". *Proc. Instn. Mech. Engrs Part G: J. Aerospace Engineering,* **217**.

[2] Taylor, G., 1923. "Stability of a viscous liquid contained between two rotating cylinders". *Philosophical Transactions of the Royal Society of London. Series A, Containing Papers of a Mathematical or Physical Character,* **223**, pp. 289–349.

[3] Farrall, M., Hibberd, S., Simmons, K., and Gorse, P., 2006. "A numerical model for oil film flow in an aeroengine bearing chamber and comparison to experimental data". *Journal of Engineering for Gas Turbines and Power*.

[4] Williams, J., 2008. "Thin film rimming flow subject to droplet impact at the surface". PhD thesis, The University of Nottingham.

[5] Kay, E., Hibberd, S., and Power, H., 2014. "A depth-averaged model for non-isothermal thin-film rimming flow". *International Journal of Heat and Mass Transfer,* **70**(Complete), pp. 1003–1015.

[6] Kakimpa, B., Morvan, H. P., and Hibberd, S., 2015. "Solution Strategies for Thin Film Rimming Flow Modelling". *ASME Paper no. GT2015-43503*.

[7] Adeniyi, A., Morvan, H., and Simmons, K., 2013. "Droplet-Film Impact Modelling Using a Coupled DPM-VoF Approach, ISABE-2013-1419". *Proceedings of XXI Intl. Symp. on Air Breathing Engines (ISABE 2013), AIAA, Busan, South Korea*.

[8] Adeniyi, A. A., Morvan, H. P., and Simmons, K. A., 2014. "A transient CFD simulation of the flow in a test rig of an aeroengine bearing chamber". *ASME Paper no. GT2014-26399*.

[9] Tkaczyk, P., and Morvan, H., 2012. SILOET: CFD Modelling Guidelines of Engine Sumps - Oil and Air Flows Simulation of Bearing Chambers & Sumps using an Enhanced Volume of Fluid (VOF) Method, JF82/PT/06, UTC in Gas Turbine Transmission Systems. Tech. rep., The University of Nottingham, UK,.

[10] Chandra, B., Simmons, K., Pickering, S., Colliocot, S., and Wiedemann, N., 2012. "Study of Gas/Liquid behaviour within an Aeroengine Bearing Chamber". *ASME Paper No. GT2012-68753*.

[11] Glahn, A., Blair, M., Allard, K., Busam, S., O.Schfer, and Wittig, S., 2003. "Disintegration of Oil Films Emerging from Radial holes in a Rotating Cylinder". *Journal of engineering for gas turbines and power,* **125**(4), pp. 1011–1020.

[12] Crouchez-Pillot, A., and Morvan, H., 2014. "CFD Simulation of an Aeroengine Bearing Chamber using an Enhanced Volume of Fluid (VOF) Method". *ASME Paper no. GT2014-26405*.

[13] Adeniyi, A. A., Morvan, H. P., and Simmons, K. A., 2015. "A multiphase computational study of oil-air flow within the bearing sector of aeroengines". *ASME Paper no. GT2015-43496*.

[14] Kannel, J., and Bupara, S., 1978. "A simplified model of cage motion in angular contact bearings operating in the ehd lubrication regime". *Journal of Tribology,* **100**(3), pp. 395–403.

[15] Gupta, P., 2012. *Advanced Dynamics of Rolling Elements*. Springer Science & Business Media.

[16] Jones, A. B., 1959. "Ball motion and sliding friction in ball bearings". *Journal of Basic Engineering, Transactions ASME, D,* **81**.

[17] Gupta, P., 1979. "Dynamics of rolling element bearings, part 1: cylindrical roller bearing analysis". *Trans. ASME, J. Lubric. Technol.,* **101**.

[18] Sum, W. W., 2005. "Dynamic analysis of angular-contact ball bearings and the influence of cage geometry". PhD thesis, The University of Nottingham.

[19] Ai, X., and Moyer, C. A., 2000. *Rolling Element Bearings Chp. 28: Modern Tribology Handbook*. CRC Press.

[20] Foord, C., 2014. "High-speed ball bearing analysis". *Proceedings of the Institution of Mechancal Engineers, Part G: Journal of Aerospace Engineering*.

[21] Wang, W.-z., Hu, L., Zhang, S.-g., Zhao, Z.-q., and Ai, S., 2014. "Modelling angular contact ball bearing without raceway control hypothesis". *Mechanism and Machine Theory,* **82**, pp. 154–172.

[22] Changqing, B., and Qingyu, X., 2006. "Dynamic model of ball bearings with internal clearance and waviness". *Journal of Sound and Vibration,* **294**.

[23] Sussman, M., and Puckett, E., 2000. "A Coupled Level Set and Volume-of-Fluid Method for Computing 3D and Axisymmetric Incompressible Two-Phase Flows". *Journal of Computational Physics,* **162**, pp. 301–337.

[24] ANSYS-Fluent, 2015. ANSYS Fluent Theory Guide.